Published as: Walter W. Focke, Heinrich Badenhorst, Shatish Ramjee, Hermanus Joachim Kruger, Riaan Van Schalkwyk, Brian Rand. Graphite foam from pitch and expandable graphite. Carbon 73 (2014) 41–50. http://dx.doi.org/10.1016/j.carbon.2014.02.035

Graphite foam from pitch and expandable graphite

Walter W Focke,* Heinrich Badenhorst, Shatish Ramjee, Hermanus Joachim Kruger, Riaan Van Schalkwyk, Brian Rand

SARChI Chair in Graphite Materials and Technology, Institute for Applied Materials, Department of Chemical Engineering, University of Pretoria, Private Bag X20, Hatfield, Pretoria 0028, South Africa

Abstract

Graphite foams were prepared from a coal tar pitch that was partially converted into mesophase. Expandable graphite was used instead of an inert gas to "foam" the pitch. The resulting foam was subjected to a series of heat treatments with the objective of first crosslinking the pitch, and thereafter carbonizing and graphitizing the resulting foam. XRD confirmed that the graphitization at 2600 °C resulted in a highly graphitic material. The porosity of this foam derives from the loose packing of the vermicular exfoliated graphite particles together with their internal porosity. During the foaming process the pitch tends to coat the outside surface of the expanding graphite flakes. It also bonds them together. The graphite foam prepared with 5 wt.% expandable graphite had a bulk density of 0.249 g cm^{-3}, a compressive strength of 0.46 MPa and a thermal conductivity of 21 W $m^{-1}K^{-1}$. The specific thermal conductivity (thermal conductivity divided by the bulk density) of this low-density carbon foam was 0.084 W $m^2kg^{-1}K^{-1}$which is considerably higher than that of copper metal (0.045 W $m^2kg^{-1}K^{-1}$) traditionally used in thermal management applications.

KEYWORDS: Graphite foam; expandable graphite; mesophase pitch

*Corresponding author: Tel: +27 12 420 3728. Fax: +27 12 420 2516. E-mail: walter.focke@up.ac.za (W.W. Focke)

1. Introduction

Carbon foams are classified as either amorphous and thermally insulating, or graphitic and thermally conductive. The first variety is generally prepared by carbonizing foamed thermoset polymers [1, 2]. The final product is typically a reticulated glassy carbon foam with a pentagonal dodecahedron structure [3] with thermal conductivities lower than 1 W $m^{-1}K^{-1}$ [4-6].

Conductive foams are important in thermal management applications and as thermal energy storage materials [2, 7]. Klett and coworkers [6-10] pioneered the fabrication of thermally conductive graphite foams from mesophase pitch. These foams have an open cell structure and feature high thermal conductivities (up to 182 W $m^{-1}K^{-1}$ at a bulk density of 0.61 g cm^{-3} [8]), low density, relatively large surface area and a low coefficient of thermal expansion [2]. The specific thermal conductivity is the thermal conductivity divided by the bulk density of the foam. Klett *et al*. [6] consider this to be an important measure for conductive graphite foams in applications where weight savings are vital. The value for copper is ca. 0.045 W $m^2kg^{-1}K^{-1}$ [6]. Graphite foams can have specific thermal conductivity values that are six times higher than that for copper.

Carbon foams can also be produced using other low-cost precursors, such as coal, coal tar pitch and petroleum pitch [11]. However, high thermal conductivity foams are not easily achieved through this approach. Mesophase pitch is the preferred raw material for graphite foam production as it can be graphitized to a thermally conductive state. In the Klett approach, the graphite foams are produced by foaming a mesophase pitch with an inert gas at high pressures [12] or by volatile gas released from the mesophase pitch itself [8]. However, Yadav et al. [2] also produced high thermal conductivity graphite foam using a sacrificial template method. They impregnated polyurethane foam with mesophase pitch and converted it into graphite foam by suitable heat treatments. Open pore structure foams with density in

the range 0.23 - 0.58 g cm^{-3}, compressive strengths in the range of 3 - 5 MPa and thermal conductivity values up to 60 W $m^{-1}K^{-1}$ were obtained.

Zhu et al. [13] showed that the compressive strength of mesophase-based foams can be improved significantly by addition of graphite flakes. Adding just 5 wt.% graphite improved the compressive strength from 3.7 MPa to 12.5 MPa. This foam had an apparent density of 0.757 g cm^{-3} and a thermal conductivity of 110 W $m^{-1}K^{-1}$.

This communication explored a different way of producing carbon foams. The foams were prepared using expandable graphite (EG) together with a coal tar pitch that was partially converted to the mesophase state. Although pure mesophase pitch is preferred for foam production it is a rare commodity. Hence coal tar pitch was selected owing to its lower cost and general availability. A key property of expandable graphite is its tendency to exfoliate when heated to high temperatures [14, 15]. During exfoliation it expands rapidly in a worm-like manner to form vermicular graphite with a low density [16-18]. The bulk density can be as low as 0.006 g cm^{-3} [19]. The exfoliation of the expandable graphite provides the "foaming" action to produce the required porosity. The purpose of the investigation was to determine the viability of this method of carbon foam fabrication and to establish whether the foams can be graphitized to a state of high thermal conductivity. Afanasov et al. [20] previously prepared exfoliated graphite-coal tar pitch composites but they did not prepare foams as in this study.

2. Experimental

2.1. Materials

The coal tar pitch (110MP) obtained from Arcelor-Mittal had a softening point of 63 °C and a coke yield of ca. 44 wt.%. The quinoline insolubles (QI) and toluene insolubles (TI) were 9 wt.% and 34 wt.% respectively. The Aromaticity Index was 0.53 and the C/H atomic ratio

was 1.83. The expandable graphite grade ES170 300A (onset temperature 300°C) was obtained from Qingdao Kropfmuehl Graphite (China). According to the manufacturer, it produces > 170 mL/g exfoliated material when heated to well above 300 °C. Natural flake graphite sourced from Zimbabwe was supplied by BEP Bestobell (South Africa) and characterized for comparison purposes.

2.2. Sample preparation

2.2.1. Preparation of mesophase pitch

The Arcelor-Mittal pitch was heat treated in a vertical tube furnace at a temperature of 437 °C for 6 h in a nitrogen atmosphere to prevent oxidation. A solid sample of pitch was taken from the crucible after the heat treatment. This sample was cast in epoxy resin and cured for 4 h at 60 °C. This resin-encased sample was polished for study with the optical microscope under polarized light. The rest of the heat-treated pitch containing mesophase was ground into a fine powder for further experiments and characterization purposes.

2.2.2. Preparation of the graphite foams

The carbon foam samples were prepared in small stainless steel tubes with a diameter of 35 mm and height of 40 mm. The mesophase-containing pitch powder was dry mixed with different amounts of expandable graphite. The mixed powdered samples were then loaded into the stainless steel tubes and covered with aluminum foil and placed in a muffle furnace for 15 min. The mixtures were all foamed at the same furnace temperature of 460 °C in an air atmosphere. The foams were allowed to cool down before they were pressed out of the tubes. Depending on the EG content, the loaded mass was varied so that the foam did not rise above the tube exit. For example, for the foam made with 5 wt.% EG the loaded mass was 9.5 g. They foams were then partially cross linked by heating them in air at 250 °C for 20 h in a

muffle furnace. This fixed the structure of the foam and prevented its collapse during subsequent heat treatments. Next the samples were carbonized in a nitrogen atmosphere. The temperature was raised at 50 K min^{-1} to 1000 °C and soaked at this temperature for 1 h. Finally the foams were graphitized in a helium atmosphere in a graphitizing furnace (GT Advanced Technologies (previously Thermal Technology Inc.), Graphite Hot Zone Laboratory Furnace Model 1000-2560-FP20). The temperature was increased at a rate of 60 K min^{-1} up to 2600 °C and soaked at this temperature for 1 h before cooling down.

2.3. Characterization

2.3.1 Graphite particle size, BET surface area and density determination

The graphite particle size distributions were determined with a MastersizerHydrosizer 2000MY (Malvern Instruments, Malvern, UK). The specific surface areas of the graphite powders were measured on a Micromeritics Flowsorb II 2300 and a Nova 1000e BET instrument in N_2 at 77 K. Densities were determined with a Micrometrics AccuPyc II 1340 helium gas pycnometer.

2.3.2. Thermogravimetry (TGA)

A Mettler Toledo A851 simultaneous TGA/SDTA machine was used for thermogravimetric analysis. Powder samples (ca. 20 mg) were placed in open 70 μL alumina pans and heated from 25 °C to 1000 °C at a scan rate of 10 K min^{-1} in air or nitrogen flowing at a rate of 50 mL min^{-1}.

2.3.3. Thermomechanical analysis

The softening points of the pitch samples and the thermal expansion of the expandable graphite were measured on a TA instruments Q400 Thermo Mechanical Analyzer. Sufficient

graphite powder was placed in an alumina sample pan such that the bed height was between 35 μm and 40 μm. The flake expansion behavior was measured with a flat-tipped standard expansion probe using an applied force of 0.02 N. The temperature was scanned from 30 °C to 1000 °C at a scan rate of 10 K min^{-1} in nitrogen atmosphere. The expansion relative to the original powder bed height is reported.

The softening point of the pitch samples was determined with the penetration probe using an applied force of 0.005 N. The temperature was scanned from 30 °C to 400 °C at a scan rate of 2.5 K min^{-1} in a nitrogen atmosphere.

2.3.4. Dynamic mechanical analysis (DMA)

DMA data were recorded on a Perkin Elmer DMA 8000 using material pockets [21]. The latter are stainless steel envelopes that hold powdered samples so that they can be mounted in the DMA instrument. Measurements were done in the single cantilever bending mode. The temperature ramp rate was 2 K min^{-1} and a frequency of 1 Hz was employed for all measurements.

2.3.5. Rheometry

The effects of shear rate and temperature on the viscosity of the heat-treated pitch were determined with an Anton Paar Physica MCR301 rheometer fitted with a CTD600 convection hood for temperature control. Data were obtained in the steady shear mode using a 20 mm parallel plate measuring system. The temperature was varied from 250 °C to 280 °C and the shear rate between 0.01 and 10 s^{-1}. Nitrogen gas was used to maintain an inert atmosphere.

2.3.6. Optical microscopy (OM)

The microstructure of the heat-treated pitch and the foams was studied with optical microscopy (OM) under reflecting and polarized light using a Leica DM 2500M microscope. Samples mounted in an epoxy resin were polished with a Buehler Alpha 2 speed polisher. The polishing was done under a continuous flow of water for one minute each on a succession of increasingly finer silicon carbide abrasive papers (400, 600, 1200 grit). Finally the sample polishing was completed using first a 1 µm and then a 0.05 µm Buehler MetaDi polishing suspension for 3 and 2 minutes, respectively.

A fracture surface of the graphitized foam, made with 5 wt.% expandable graphite, was also studied using a Zeiss Discovery V20 stereo microscope.

2.3.7. Scanning electron microscopy (SEM)

Scanning electron microscope (SEM) images were obtained using an ultrahigh resolution field emission SEM (HR FEGSEM Zeiss Ultra Plus 55) with an InLens detector at an acceleration voltage of 1 kV to ensure maximum resolution of surface detail.

2.3.8. Raman spectroscopy

The Raman spectra were recorded with a T64000 series II triple spectrometer system from HORIBA Scientific, Jobin Yvon Technology using the 514.3 nm laser line of a coherent Innova®70 Ar^+ laser with a resolution of 2 cm^{-1} in the range 1200 to 1700 cm^{-1}. The samples were recorded in a backscattering configuration with an Olympus microscope attached to the instrument (using a LD 50x objective). The laser power was set at 6 mW and a nitrogen-cooled CCD detector was used. The accumulation time was 120 s and the spectra were baseline corrected with using LabSpec software.

2.3.9. X-Ray diffraction (XRD)

XRD diffraction patterns were recorded using a Bruker D8 Advance powder diffractometer fitted with a Lynx eye detector. Measurements were performed in the 2θ range 15° – 120° with a 0.04° step size and a counting time of 0.2 s. The interlayer spacing, d_{002}, calculated using the Bragg equation, was used as an indicator for the extent of ordering.

2.3.10. Thermal diffusivity

The thermal diffusivities of the foams were estimated from the dynamic temperature response curves measured using an experimental setup employing heat flux sensors. Details of the method are provided in the Supplementary material. The thermal conductivity values for the graphitized foams were calculated from the measured density and thermal diffusivity values using the following equation

$$k = \alpha \rho C_p \quad (1)$$

where, k is the thermal conductivity (W $m^{-1}K^{-1}$); α = Thermal diffusivity (m^2s^{-1}); ρ is the density (kg m^{-3}); and C_p is the specific heat (J $kg^{-1}K^{-1}$), (assumed to be 713 J $kg^{-1}K^{-1}$ [6, 8]).

2.3.11 Mechanical compression tests

The compressive strength of cylindrical foam samples was determined in the expansion direction. The samples had a diameter of 33 ± 1 mm and a height of at least 35 mm. The crush tests were performed on a Model 4303 Instron machine fitted with a 1 kN load cell. The compressive load rate was 30 mm min^{-1}. The overall shapes of the stress strain curves were consistent with those found for other porous carbon foams, i.e. the stress increased rapidly to a crush initiation value after which it flat-lined [22]. The crush point was reached at a stroke distance of about 1 mm (2% strain). The mean crush stress was estimated from the plateau

values measured at stroke distance between 2 mm and 6 mm, i.e. 4 – 17% strain for three different samples.

3. Results and Discussion

3.1 Expandable and exfoliated graphite characteristics

The particle size, BET surface area, and densities of the expandable graphite sample are presented in Table 1. The surface area of the expandable graphite samples increased by a factor of about twenty two when it expanded on heat treatment at 600 °C. Fig. 1 shows that the exfoliated graphite has a worm-shaped, accordion-like structure. Slit-shaped gaps between the graphite platelets are clearly visible in the hi-resolution micrograph.

The accordion-like vermicular microstructure of the expanded graphite is built up of distorted graphite sheets that mostly retain their original lateral dimensions. The average thickness of these sheets can be estimated from the BET surface area using the equation

$$t = 2/\rho A \qquad (2)$$

Where t is the average sheet thickness in m, ρ is the density of graphite in kg m^{-3}; and A is the BET surface area in m^2 kg^{-1}. Note that equation (2) neglects the edge surface area of the flakes. Applying this equation to the expanded graphite sample yields average flake thicknesses of about 60 nm. This confirms the nanostructured nature of the expanded "worms".

A key property of expandable graphite is its ability to exfoliate in a narrow temperature range. Fig. 2 visualizes the TGA mass loss and the TMA expansion occurring during the exfoliation process. The TGA trace indicates a single-step exfoliation event with an onset temperature above 250 °C. By 600 °C the sample has lost 10% of it mass owing to the CO_2 and SO_2 gas released during the exfoliation. The TMA onset temperature for the

exfoliation is about 300 °C. However, the TGA curve shows that mass loss commences at a lower temperature.

Fig. 3 shows the XRD diffractograms for the expandable graphite in neat and exfoliated form and compares these to the diffractogram for the natural flake graphite. Table 2 lists the *d*-spacings calculated from the positions of the main reflections observed in the diffractograms. The *d*-spacing for the natural graphite was 0.335 nm. The diffractograms of the expandable graphite in the neat and exfoliated form showed a reflection that corresponds to the same *d*-spacing. The neat expandable graphite sample also features an additional reflection located at a lower angle. This reflection is due to the sulfuric acid intercalated graphite phase. After exfoliation, it disappears and only a pure graphite reflection is evident.

3.2. Characterization of the pitches

Following the six hour heat treatment at 437 °C, the quinoline insolubles (QI) and toluene insolubles (TI) of the coal tar pitch were 41 wt.% and 68 wt.% respectively. The coke yield increased from 44 wt.% to 73 wt.% and the C/H atomic ratio from 1.83 to 2.20.

Fig. 4 shows a polished surface of the heat-treated pitch under reflected polarized light. It shows that the pitch is a two phase system comprising mesophase spheres dispersed within a continuous phase of untransformed pitch. Domains are evident within the spheres which show different interference colors due to the interaction of their basal planes with incident polarized light [23]. Domains that appear yellow or blue are aligned perpendicular to each other. The pitch matrix has not transformed to the liquid crystal state and so displays optical isotropy under the polarized light. Fig. 4 also reveals a high concentration of quinoline insoluble particles that are aggregated around the spherical mesophase spheres. These particles originate as carbonaceous inclusions from the coking process in which the coal tar was produced. As explained in the experimental section, the QI content was determined by

solvent extraction of the raw pitch and heat treated pitches. The initial value of 9 wt.% increased to 41 wt.% after heat treatment. The presence of these particles is known to restrict coalescence of the mesophase spheres into larger drops. The mesophase content was estimated at 49 volume% from image analyses.

A TGA run was performed in a nitrogen atmosphere on the heat-treated pitch to determine the carbon yield (Fig. 5). Mass loss commenced at 200 °C and reached a plateau value above 600 °C, This corresponds to a carbon yield of approximately 73% for the heat-treated pitch.

Fig. 6 shows the TMA data and the tan δ plots obtained with the DMA for the neat pitch and the heat-treated pitch. The glass transition (Tg) values were taken as the temperatures corresponding to maxima in the tan δ curves. In this context, the heat treatment raised the glass transition temperature by almost 40 °C from 74 °C for the neat pitch to 113 °C for the heat-treated pitch. The corresponding TMA-softening temperatures also shifted by 40 °C from ca. 63 °C for the neat pitch to 103 °C for the heat-treated pitch.

Fig. 7 reports the effect of temperature and shear rate on the shear viscosity of the heat-treated pitch. It shows that the pitch exhibited strong shear thinning behavior. This is assumed to be due to shear induced droplet deformation and breakdown of agglomerates of the mesophase droplets. That deformation of mesophase spheres into oblate spheroids can take place under shear was previously demonstrated by Collett and Rand, albeit at higher temperatures [24].

3.3 Characterizations of the foam samples

Mixtures of mesophase powder and expandable graphite (EG) were made starting at 1 wt.% EG and increasing in 1 wt.% increments up to 10 wt.% EG. The 1% mixture did not really produce a foamed structure and looked more like a piece of solid mesophase while the 10

wt.% EG mixture produced foam that had little structural integrity. Homogeneous foams were obtained for samples that contained 3, 4 and 5 wt.% EG. Mixtures containing higher concentrations of EG produced foams that were not homogenous with the top layer being less dense than the bottom part of the foam. The compressive strength of the foam made with 5 wt.% EG was 0.46 ± 0.04 MPa. At a comparable density, this value compares favorably with those found for the graphite foams investigated by Smith et al. [22]. However, the compressive strength is significantly lower than values reported by other authors [2, 11, 13, 25].

Fig. 8 shows photographs of a green (i.e., as produced and before crosslinking and carbonization) and a graphitized foam sample obtained with the addition of 5 wt.% expandable graphite. Fig. 9 shows a close-up of the microstructure of this foam. It illustrates that the porosity of the foam derives from the loose packing of the flexible "worms" as well as the porosity within these "worms". Thus the porosity is not uniform and there is a wide distribution of pore dimensions. The outer surfaces of the graphite "worms" appear to be coated by a thin layer of residual pitch. However, regions rich in pitch are also visible. When the foam is cut or fractured, it is found that the "worms" are not strongly bound to the pitch network and easily drop out. This is significant for the conductivity results presented later.

Scanning electron micrographs of the foams at various stages of the heat treatment protocol, i.e. as (A & B) "green" (i.e. as prepared and before carbonization), (C & D) carbonized and (E & F) graphitized foams are shown in Fig. 10. The figures show the pitch surface coating on the graphite "worms" since the layered nature of the EG visible in Fig. 1 is obscured. The "green" samples have a high prevalence of spherical particles embedded in the pitch layer as seen in Fig. 10B. These appear to be the mesophase spheres which are clearly visible in the polarized light optical micrograph of the 'green" foam material shown in Fig. 11A. The carbonized micrographs displayed do not show any evidence of the isotropic phase

that is present in the “green” sample. This indicates that the stabilization process did not fully cross link the pitch and the isotropic phase has subsequently transformed to mesophase during heat treatment.

Fig. 11A shows a typical polarized micrograph of the “green” foam after oxidative stabilization. The exfoliated graphite is evident and there is no evidence of any dispersion of the exfoliated graphite layers, the expanded, concertina-like morphology being retained as observed in the SEM micrographs shown above (Fig. 1). The presence of mesophase domains is clearly evident but they are not fully coalesced, being restricted by the QI particulates as discussed in the sections above, the effect being one resembling grain boundaries in polycrystalline materials. However close inspection reveals that the isotropic phase has been retained, ‘locked-in’ as it were, by the oxidative stabilization process. This is even more evident in the micrographs of carbonized materials in Fig. 11B. The two phase nature is discernible in this image. Close inspection reveals that around the edges of pores the mesophase spheres have been deformed by the local bi-axial stresses that prevail during bubble expansion. That deformation and preferred orientation within thin ligaments is shown more clearly in Fig. 11C which is from the graphitized product.

These images reveal that the foams are in fact multi-phase comprising the porous expanded graphite regions poorly bonded into the pitch-derived matrix which itself comprises graphitized and non-graphitized phases emanating from the two phase nature of the precursor pitch along with extensive macroporosity resulting from the foaming of the pitch and the exfoliation of the expandable graphite.

Thus the graphite foams are basically an interconnected network of ligaments containing dispersed expanded “worms” within a matrix that is predominately graphitic deriving from the mesophase but with substantial continuous regions of optically isotropic and hence non-graphitized carbon deriving from the isotropic phase in the precursor that was

'locked-in; during the oxidation stage. During the foaming process the EG and mesophase pitch powder are heated up simultaneously. The pitch starts to soften at a temperature well below the temperature where the EG starts to expand as shown by the glass transition temperature measurements and the rheology data. When the EG exfoliates, the "worms" that form are covered by a thin film of pitch. This pitch coating forms the basis of the bulk interconnected structure. If the mesophase pitch is sufficiently fluid the mesophase domains can deform and align to some extent parallel to the surface of the "worms" and especially along the ligaments during the rapid expansion, as shown in Fig. 11C. In this case however the domain size of the mesophase is limited by the QI phase and better results could probably be achieved by using a synthetic pitch which is 100% mesophase. However, the higher softening point and higher viscosity might prevent the formation of an even coating of the EG particles when they exfoliate or even restrict the exfoliation process itself.

The mass and the dimensions of the foams were measured before and after each heat treatment step. There were basically no differences in the mass loss results obtained for samples made with 3 wt.%, 4 wt.% and 5 wt.% expandable graphite. For these the average mass loss from "green" foam to carbonized and from "green" to graphitized foam were 17.3 ± 0.5 wt.% and 20.1 ± 0.8 wt.% respectively. The volume shrinkages from "green" foam to carbonized foam and from "green" foam to graphitized foam, for the sample made with 5 wt.% EG, were 16.9 ± 1.4% and 19.1 ± 1.4% respectively. This compares favorably with the high volume shrinkage of > 50% observed for foams derived from mesophase pitch using the template method [2].

Fig. 12 shows the effect of EG content on the bulk density of the graphitized foam samples. The bulk density of the graphitized foam prepared with 5 wt.% expandable graphite was 0.249 g cm^{-3}. Considering the volume expansion of the neat expandable graphite (175 mL g^{-1}), the volume shrinkage of the foam and the mass losses on heat treatment, the

theoretical lower limit for the foam bulk density is estimated at 0.112 g cm^{-3}. This implies that the presence of the viscous liquid pitch must have impeded the expansion of the expandable graphite during the foaming process.

Fig. 13 shows the XRD diffractograms for the foam samples. All the samples show the characteristic d_{002} graphite reflection at ca. 30.9° (CoKα). See Table 2. In the "green" and carbonized foams the origin of this reflection lies in the presence of the exfoliated EG. See Fig. 3 for confirmation. The initial peak of the "green" foam is due to the fact that it already contains some expandable graphite. The broad features in the diffractograms of these foams indicate the disordered nature of the pitch phase at this stage. However, the intensity of this reflection has increased dramatically in the graphitized foam. This indicates a highly graphitized nature of the final product. Surprisingly the value of d_{002} is higher in the graphitized foam than in carbonized foam. However, the differences are small and could be attributed to experimental error. Another possible explanation is as follows: The d_{002} value in the carbonized foam is due to the exfoliated graphite phase. Once graphitized, the graphitic phase derived from the pitch (major part of the composition) dominates owing to the fact that it represents the bulk of the mass present (ca. 96 wt.%). Thus the d_{002} reflection for this, less ordered graphite phase is observed. Note that this also explains the broad nature of the peak compared to that of the graphite phase of the exfoliated expandable graphite.

Table 3 lists measured thermal diffusivities (measured in the foam rise direction) and bulk densities together with calculated thermal conductivities and specific thermal conductivity of the foam sample obtained after graphitization. Recall that the thermal conductivity of conventional glassy carbon foam is usually less than 1 W $m^{-1}K^{-1}$ [4] [5] [6]. Table 3 shows that even the "green" foam featured a thermal diffusivity that was an order of magnitude higher. This is attributed to the highly graphitic nature of the vermicular exfoliated graphite phase that forms the 3-D network in these novel foams. Carbonization improves this

value slightly but it increases by almost an order of magnitude when the foam is graphitized. This suggests a microstructure in the foam that facilitates efficient heat transfer through the network. Interestingly the specific thermal conductivity of the graphitized foam in the expansion direction (0.084 W $m^2kg^{-1}K^{-1}$) is almost double that of the reference graphite and that of copper metal (both at 0.045 W $m^2kg^{-1}K^{-1}$). This value may be compared to those obtained for pure mesophase pitch-derived foams prepared by Yadav *et al*. [2] (0.103 W $m^2kg^{-1}K^{-1}$) and Klett *et al*. [6] (> 0.27 W $m^2kg^{-1}K^{-1}$). The lower value for the present foam can be accounted for by the fact that the matrix material is not completely graphitized. It shows evidence of an optically isotropic phase emanating from the straining pitch and 'locked-in' by the oxidation process and also by the observation that the expanded graphite regions are not well bonded into the matrix. Thus the contribution that was expected from the graphite filler phase has probably not been achieved during this exploratory investigation.

5. Conclusions

A highly thermally conductive (k = 21 W $m^{-1}K^{-1}$) low-density (ρ = 0.249 g cm^{-3}) and inexpensive carbon foam was successfully prepared from a heat treated, partially mesophase coal tar pitch and an expandable graphite with a high exfoliation onset temperature. The starting pitch had a TMA softening point of 63 °C, a DMA (1 Hz) Tg of 74 °C and a coke yield of ca. 40 wt.%. It was partially converted to mesophase by a 6 h heat treatment at 437 °C. This increased the softening point to 103 °C, the Tg to 113 °C and the coke yield to 73%. The exfoliation onset temperature of the expandable graphite used was ca. 300 °C, well above the softening temperature of the mesophase pitch matrix. The foams were prepared by exposing mixtures of the finely pulverized pitch and the graphite flakes to a temperature of 460 °C for 15 min. The foams were then subjected to heat treatments involving shape stabilization, carbonization and graphitization. Cross-linking occurred via a heat treatment in

air at 250 °C for 20 h. Carbonization was conducted in a nitrogen atmosphere at a temperature of 1000 °C. Finally graphitization was effected in a helium atmosphere at 2600 °C for 1 h. Optical and scanning electron microscopy revealed that the porosity of the foams derived from both the loose packing of the wormlike exfoliated graphite particles and their own internal porosity after exfoliation. The results indicate that the pitch phase formed a thin coating on the outer surfaces of these expanded "worms" and that it bonded them into a three-dimensional structure.

The XRD of the graphite foam prepared with 5 wt.% expandable graphite featured a sharp reflectance at 20.83° (CoKα) with d_{002} = 0.337 nm in XRD pattern which reveals that the foams were highly graphitized although optical microscopy revealed a residual amount of optically isotropic phase. This foam had a bulk density of 0.249 g cm^{-3}, compressive strength of 0.46 MPa and a thermal conductivity of 21 W $m^{-1}K^{-1}$. The specific thermal conductivity (thermal conductivity divided by the bulk density) of this carbon low-density foam was 0.084 W $m^2kg^{-1}K^{-1}$, almost twice that for copper metal (0.045 W $m^2kg^{-1}K^{-1}$) traditionally used in thermal management applications.

Acknowledgements

This work is based upon research supported by the South African Research Chairs Initiative of the Department of Science and Technology (DST) and the National Research Foundation (NRF). Any opinion, findings and conclusions or recommendations expressed in this material are those of the authors and therefore the NRF ad DST do not accept any liability with regard thereto.

References

[1] Mukhopadhyay SM, Mahadev N, Joshi P, Roy AK, Kearns KM, Anderson DP. Structural investigation of graphitic foam. Journal of Applied Physics. 2002;91(5):3415.
[2] Yadav A, Kumar R, Bhatia G, Verma GL. Development of mesophase pitch derived high thermal conductivity graphite foam using a template method. Carbon. 2011;49(11):3622-30.
[3] Kuhn J, Ebert HP, Arduini-Schuster MC, Büttner D, Fricke J. Thermal transport in polystyrene and polyurethane foam insulations. International Journal of Heat and Mass Transfer. 1992;35(7):1795-801.
[4] L.J. Gibson MFA. Cellular solids: structures and properties. New York: Pergamon Press; 1988.
[5] Doermann D, Sacadura JF. Heat transfer in open cell foam insulation. Journal of Heat Transfer. 1996;118(1):88-93.
[6] Klett J, Hardy R, Romine E, Walls C, Burchell T. High-thermal-conductivity, mesophase-pitch-derived carbon foams: Effect of precursor on structure and properties. Carbon. 2000;38(7):953-73.
[7] Gallego NC, Klett JW. Carbon foams for thermal management. Carbon. 2003;41(7):1461-6.
[8] Klett JW, McMillan AD, Gallego NC, Walls CA. The role of structure on the thermal properties of graphitic foams. Journal of Materials Science. 2004;39(11):3659-76.
[9] Klett JW, McMillan AD, Gallego NC, Burchell TD, Walls CA. Effects of heat treatment conditions on the thermal properties of mesophase pitch-derived graphitic foams. Carbon. 2004;42(8–9):1849-52.
[10] Gaies D, Faber KT. Thermal properties of pitch-derived graphite foam. Carbon. 2002;40(7):1137-40.
[11] Chen C, Kennel EB, Stiller AH, Stansberry PG, Zondlo JW. Carbon foam derived from various precursors. Carbon. 2006;44(8):1535-43.
[12] Anderson HJ, Anderson DP, Kearns KM. Microcellular pitch-based carbon foams blown with helium gas. p. 756-62.
[13] Zhu J, Wang X, Guo L, Wang Y, Wang Y, Yu M, et al. A graphite foam reinforced by graphite particles. Carbon. 2007;45(13):2547-50.
[14] Furdin G. Exfoliation process and elaboration of new carbonaceous materials. Fuel. 1998;77(6):479-85.
[15] Celzard A, Marêché JF, Furdin G. Modelling of exfoliated graphite. Progress in Materials Science. 2005;50(1):93-179.
[16] Wissler M. Graphite and carbon powders for electrochemical applications. Journal of Power Sources. 2006;156(2):142-50.
[17] Chung DDL. Exfoliation of graphite. Journal of Materials Science. 1987;22(12):4190-8.
[18] Chung DDL. Review: Graphite. Journal of Materials Science. 2002;37(8):1475-89.
[19] Inagaki M. On the formation and decomposition of graphite-bisulfate. Carbon. 1966;4(1):137-41.
[20] Afanasov IM, Morozov VA, Kepman AV, Ionov SG, Seleznev AN, Tendeloo GV, et al. Preparation, electrical and thermal properties of new exfoliated graphite-based composites. Carbon. 2009;47(1):263-70.
[21] Mahlin D, Wood J, Hawkins N, Mahey J, Royall PG. A novel powder sample holder for the determination of glass transition temperatures by DMA. International Journal of Pharmaceutics. 2009;371(1-2):120-5.

[22] Smith CE, Gyekenyesi AL, Singh M, Bail J. Compressive behavior of conductive graphite foams. Journal of Materials Engineering and Performance. 2012;21(8):1703-7.
[23] Edwards IAS. Structure in Carbons and Carbon Forms. In: Marsh H, ed. Introduction to Carbon Science. London: Butterworths 1989, p. 1-36.
[24] Collett GW, Rand B. Thixotropic changes occurring on reheating a coal tar pitch containing mesophase. Carbon. 1978;16(6):477-9.
[25] Eksilioglu A, Gencay N, Yardim MF, Ekinci E. Mesophase AR pitch derived carbon foam: Effect of temperature, pressure and pressure release time. Journal of Materials Science. 2006;41(10):2743-8.

LIST OF TABLES

LIST OF FIGURES

Fig. 5 – TGA traces in N_2 for the heat-treated pitch and the "green" foam.

Fig. 6 – Thermomechanical (TMA) penetration data (open symbols) and dynamic mechanical (DMA) tan δ characterization (solid symbols) of neat pitch (○ & ●) and heat-treated pitch (▲ & △) samples. The DMA data were obtained at a frequency of 1 Hz. The softening point of the pitch samples determined with the TMA fitted with a penetration probe and using an applied force of 0.005 N.

Fig. 7 – The effects of temperature and shear rate on the viscosity of the heat-treated pitch.

Fig. 8 – Photographs of "green" graphitized foam samples obtained with the addition of 5 wt.% expandable graphite.

Fig. 9 – Stereomicroscope photograph showing the microstructure of a graphitized foam sample obtained with the addition of 5 wt.% expandable graphite.

Fig. 10 – SEM micrographs of the foams. A & B. "Green" foam; C & D. Carbonized foam; and E & F. Graphitized foam

Fig. 11 – Optical micrographs with a polarizing filter of foams taken at 50X magnification. A. "Green" foam; B. Carbonized foam; and C. Graphitized foam.

Fig. 12 – The effect of expandable graphite addition on the bulk density of the foams after graphitization.

Fig. 13 – XRD diffractograms for the foam samples obtained at various heat treatment stages.

Table 1 – Physical properties of the expandable graphite powder and its exfoliated form

Graphite sample	D_{10}, µm	D_{50}, µm	D_{90}, µm	Surface area, m^2/g	Density, g/cm^3
Neat	313	533	807	0.66	2.23 ± 0.01
Exfoliated	-	-	-	14.84 ± 0.14	-

Table 2 – XRD *d*-spacing values and Raman I_D/I_G ratios.

Sample	XRD d_{002}, nm	Raman I_D/I_G
Natural graphite	0.335	0.12
ES170 300A	0.342[a]	0.26
	0.335	
ES170 Expanded	0.337	0.10
Pitch (MP110)	–	0.61
Green foam	0.336	–
Carbonized foam	0.335	–
Graphitized foam	0.337	–

[a] Reflection due to the sulfuric acid intercalated graphite phase.

Table 3 – Measured density (ρ) and thermal diffusivity (α) measured in the foam rise direction; calculated thermal conductivity (k) and specific thermal conductivity (k/ρ) of foam samples made with 5 wt.% expandable graphite.

Sample	**$\alpha \times 10^6$, m^2s^{-1}**	**ρ, kg m^{-3}**	**k, W $m^{-1}K^{-1}$**	**$10^3k/\rho$, W $m^2kg^{-1}K^{-1}$**
Green foam	35.1	387	-	-
Carbonized foam	63.2	338	-	-
Graphitized foam	118	249	21	0.084
Graphite (reference)	63.2	1808	81.4	0.081

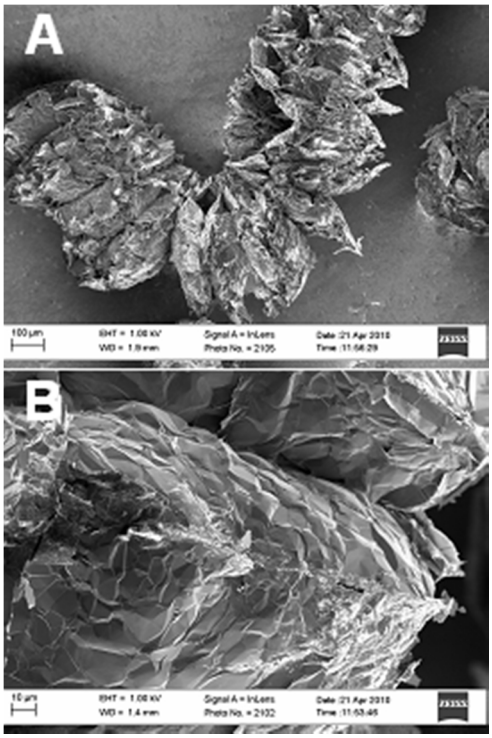

Fig. – 1 SEM micrographs of exfoliated graphite: (A) Low resolution, and (B) high resolution.

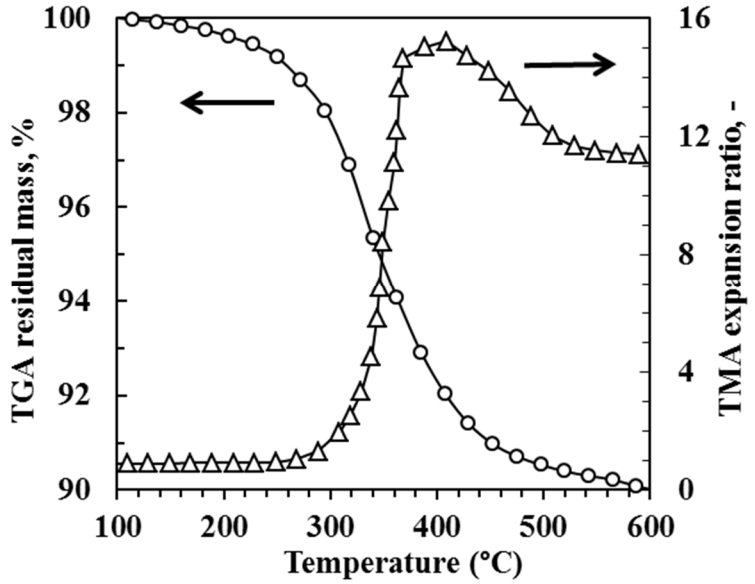

Fig. 2 – TGA traces in N_2 and TMA expansion behaviour in air for the expandable graphite.

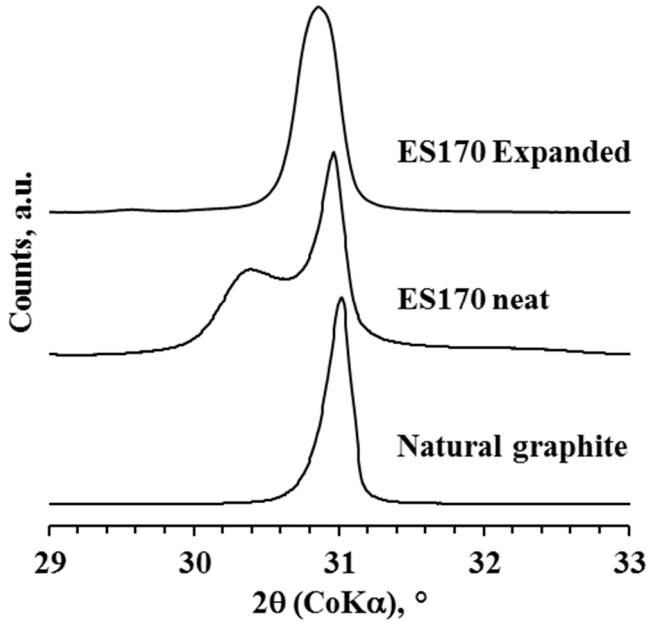

Fig. 3 – XRD patterns for the neat and exfoliated forms of the expandable graphite sample compared to that of the natural flake graphite.

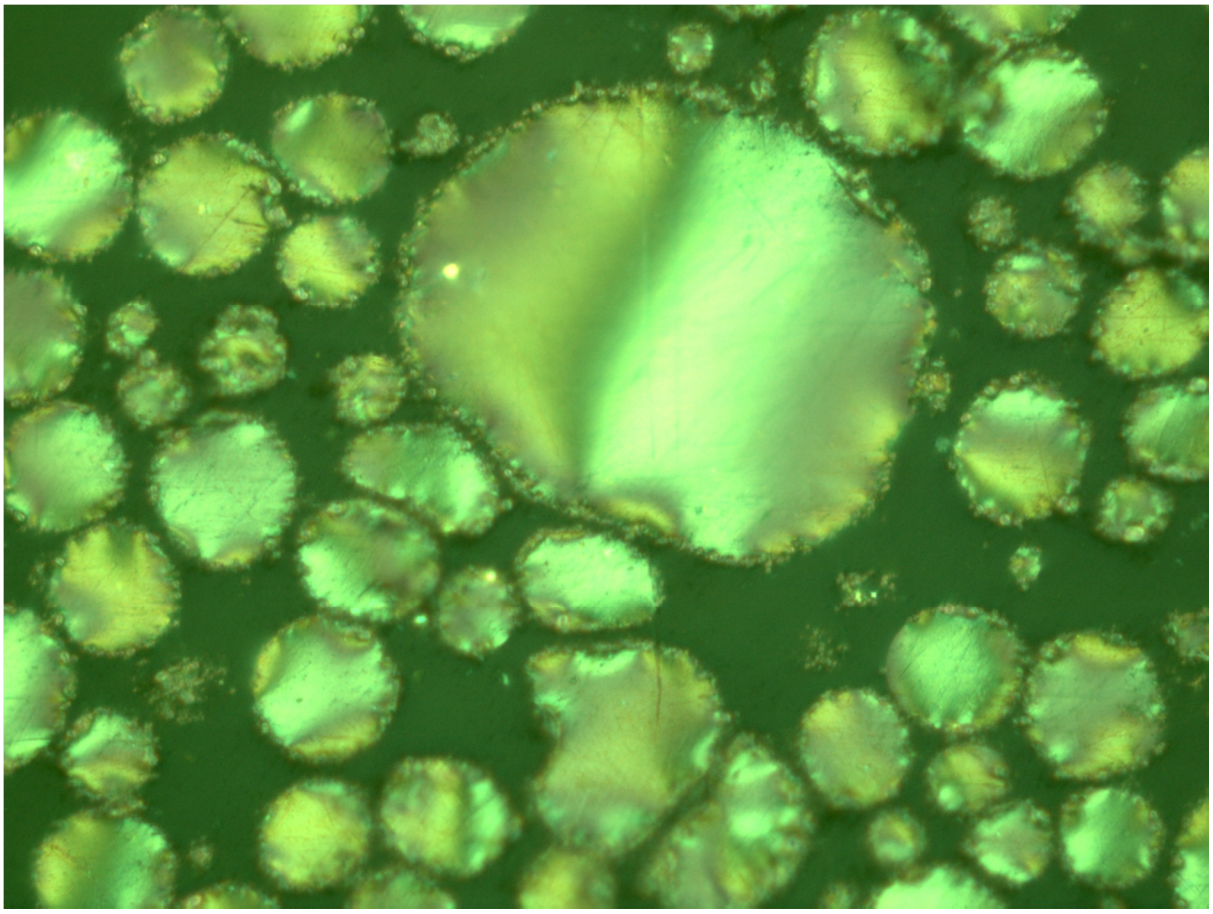

Fig. 4 – Optical micrographs of the heat-treated pitch taken, under reflecting light, at 100X magnification. The aggregation of the quinolone-insoluble particles around the edges of the mesophase spheres is clearly visible.

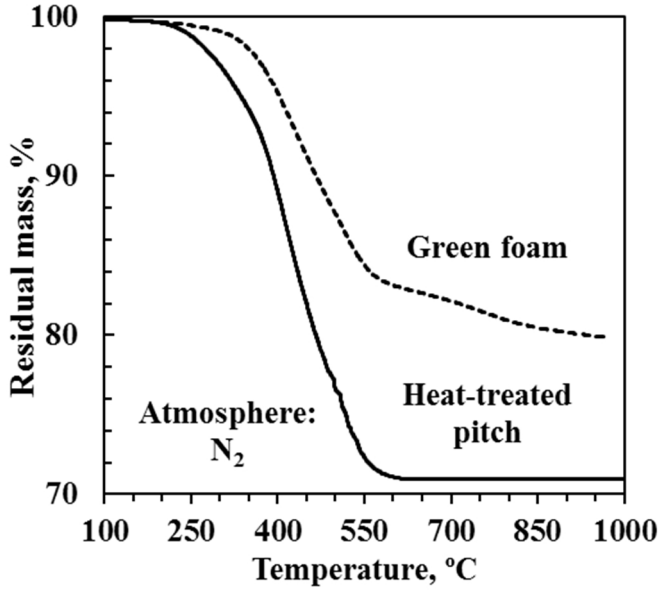

Fig. 5 – TGA traces in N_2 for the heat-treated pitch and the green foam.

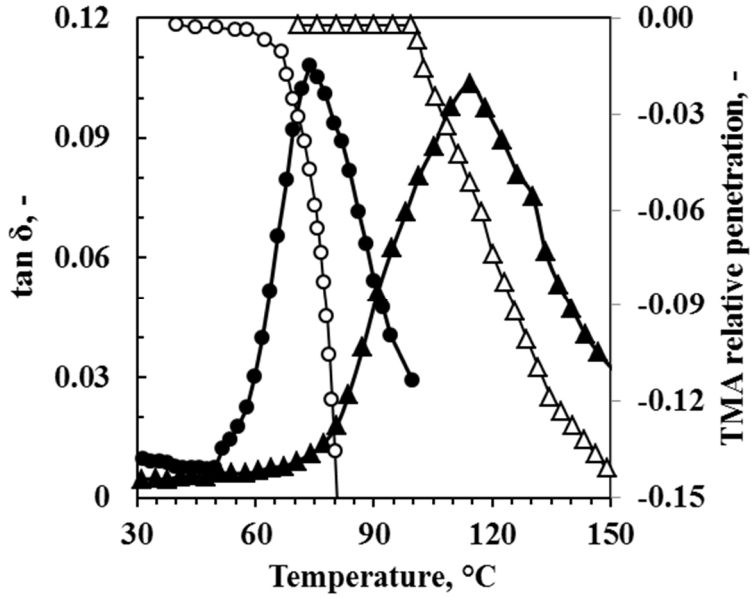

Fig. 6 – Thermomechanical (TMA) penetration data (open symbols) and dynamic mechanical (DMA) tan δ characterization (solid symbols) of neat pitch (○ & ●) and heat-treated pitch (▲ & △) samples. The DMA data were obtained at a frequency of 1 Hz. The softening point of the pitch samples determined with the TMA fitted with

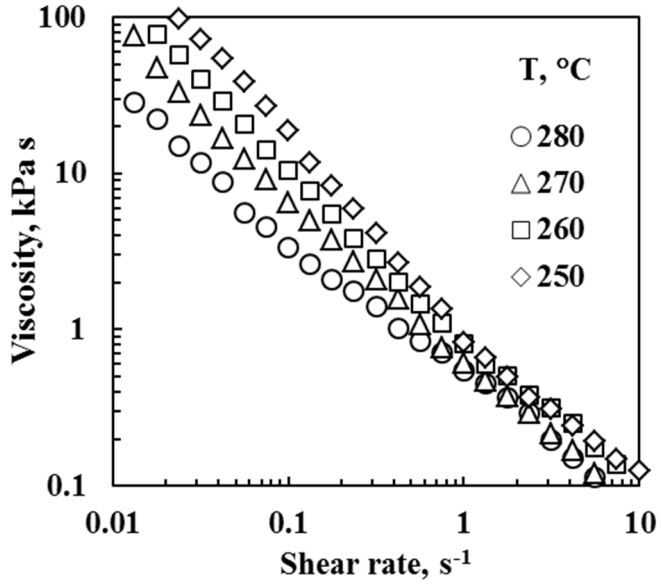

Fig. 7 – The effect of temperature and shear rate on the viscosity of the heat-treated pitch.

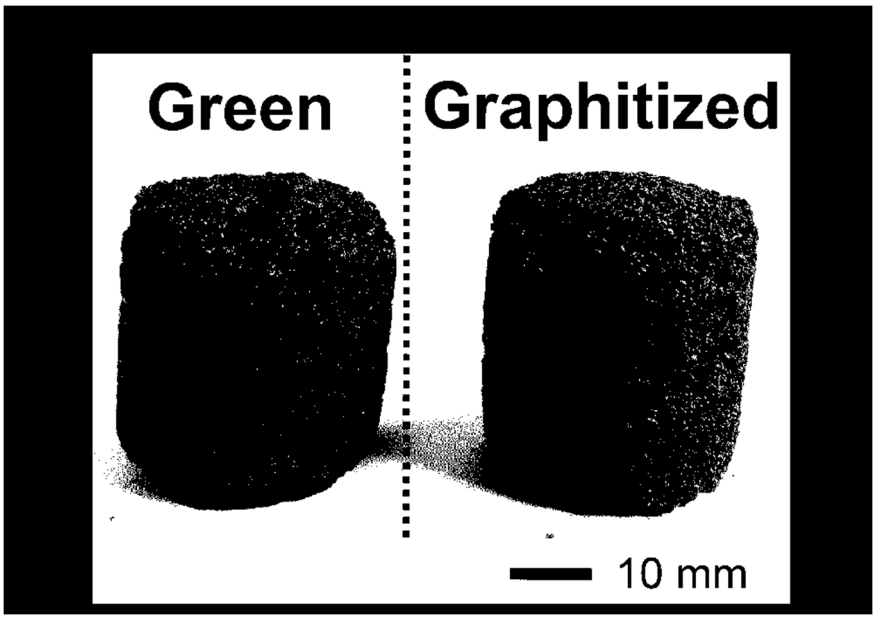

Fig. 8 – Photographs of green graphitized foam samples obtained with the addition of 5 wt.% expandable graphite.

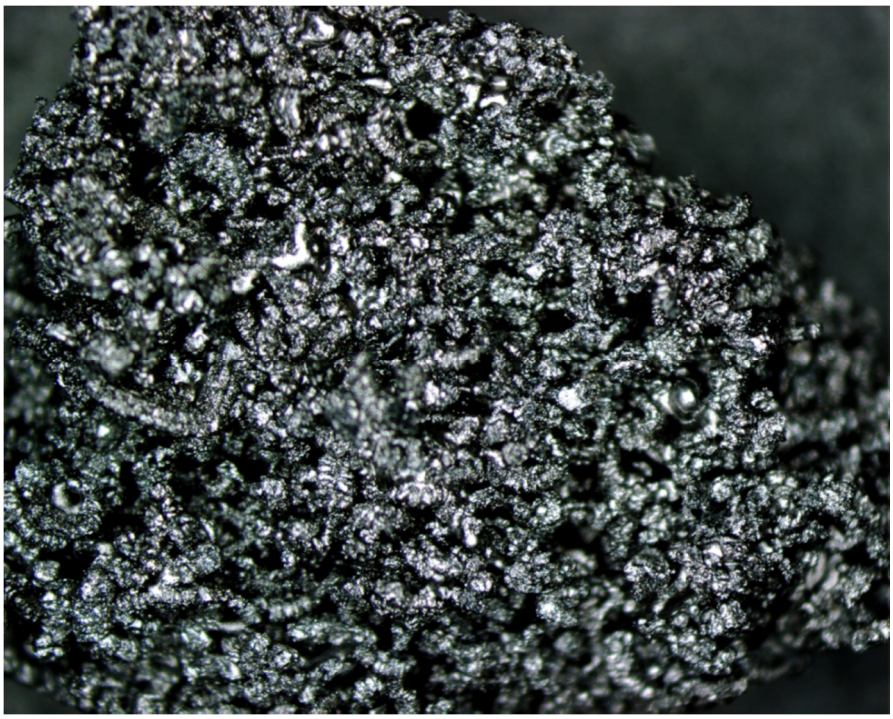

Fig. 9 – Stereomicroscope photograph showing the microstructure of a graphitized foam sample obtained with the addition of 5 wt.% expandable graphite. The width of this sample is ca. zzz mm. Need scale bar here!

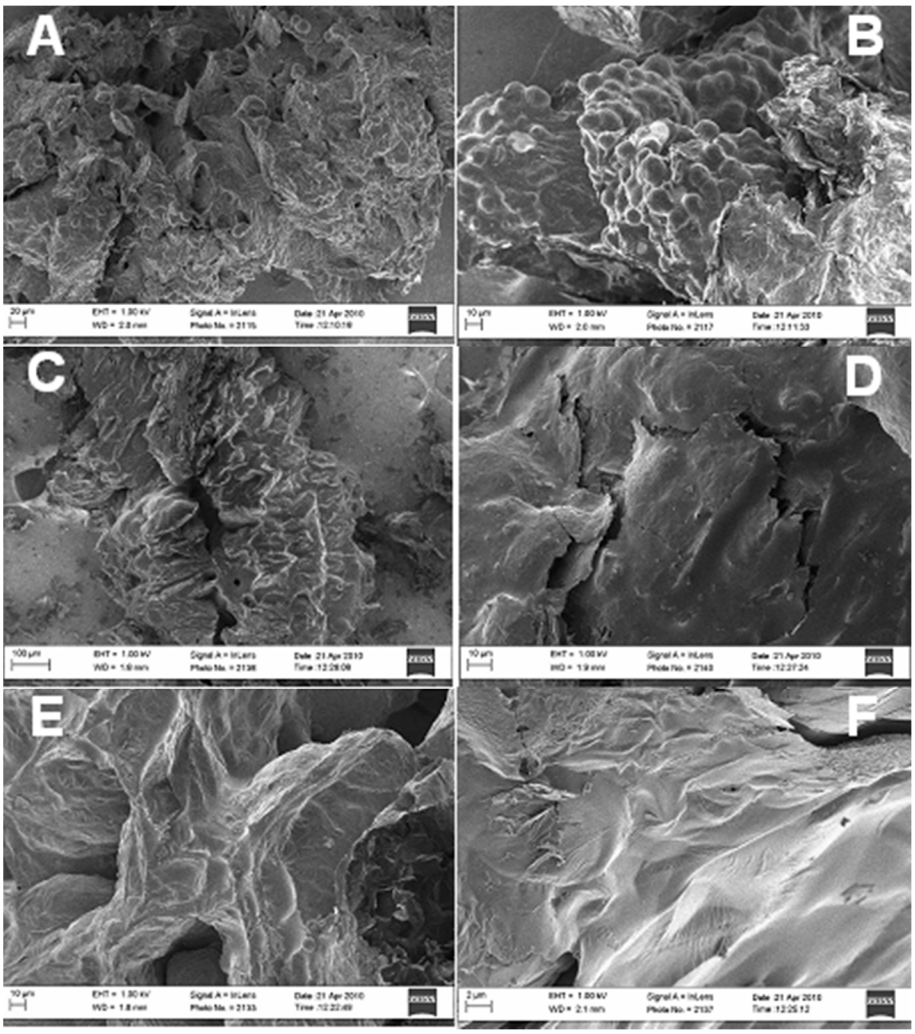

Fig. 10 – SEM micrographs of the foams. A & B. Green foam; C & D. Carbonized foam; and E & F. Graphitized foam

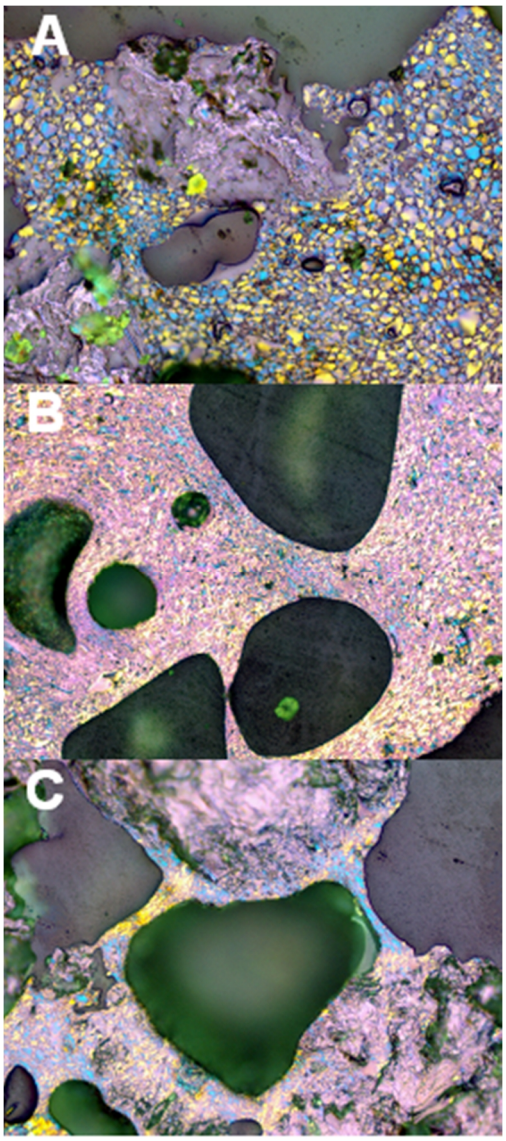

Fig. 11 – Optical micrographs with a polarizing filter of foams taken at 50X magnification. A. Green foam; B. Carbonized foam; and C. Graphitized foam.

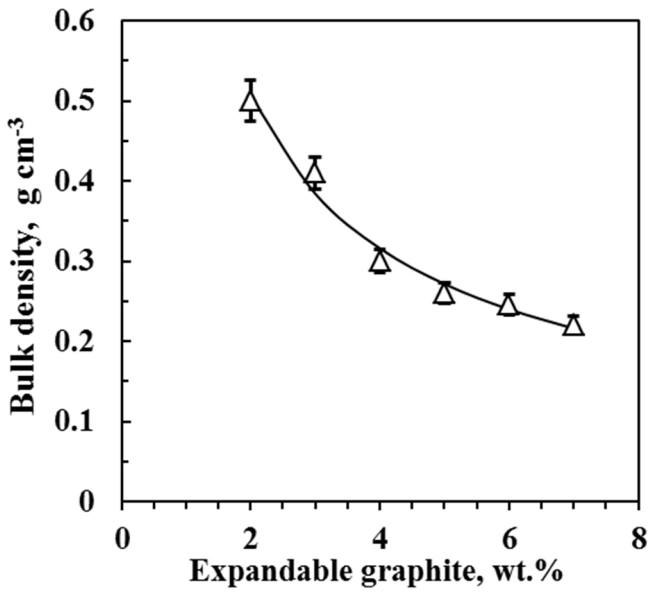

Fig. 12 – The effect of expandable graphite addition on the density of the foams after graphitization.

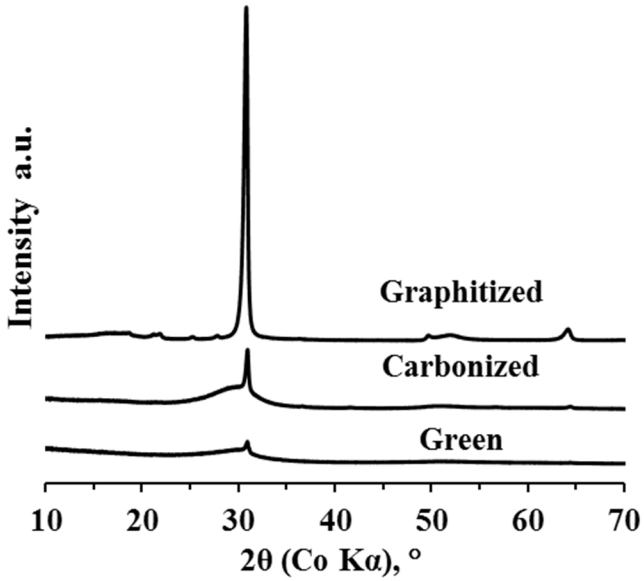

Fig. 13 – XRD diffractograms for the foam samples obtained at various heat treatment stages.